1	
2	
3	A New Dimensionless Number for Thermoelectric Generator Performance
4	Eurydice Kanimba <sup>1</sup> and Zhiting Tian <sup>1,2*</sup>
5	<sup>1</sup> Department of Mechanical Engineering, Virginia Polytechnic Institute and State University,
6	Blacksburg, Virginia 24061, USA
7	<sup>2</sup> Sibley School of Mechanical and Aerospace Engineering, Cornell University,
8	Ithaca, NY 14853, USA
9	
10	Abstract
11	Thermoelectric generators (TEG) convert heat into electricity and offer a green option fo
12	renewable energy generation. The Thomson effect has been proven to impact the overall
13	performance of TEGs negatively but is ignored in the widely-used formula for TEG maximum
14	efficiency calculation. In this study, a new dimensionless number called the Ury number (Ur) is
15	introduced to capture the influence of the Thomson effect on TEG power output and maximum
16	efficiency. Ur is defined as the ratio between the Thomson coefficient and the Seebeck coefficient
17	It is found that as Ur increases both TEG output power and maximum efficiency decrease. U
18	combined with the device figure of merit, ZT, can better dictate the overall performance of a TEG
19	

 $\hbox{$^*$ Corresponding author. Email: $z$ hitting@cornell.edu}\\$ 

#### Introduction

20

42

Thermoelectricity relies on three main principles the Seebeck, Peltier, and Thomson effects that 21 were discovered between 1821 and 1851[1]. Thermoelectric generator (TEG) devices, which 22 directly convert heat into electricity, are composed of many p-type and n-type semiconductors 23 connected in series by conducting strips that are mainly made of copper. As opposed to the 24 conventional power systems, TEGs possess some advantages including environmental friendliness 25 26 with zero CO<sub>2</sub> emission, solid-state devices without moving parts, zero noise produced during operation, and scalable from a small to a giant heat source. Maximizing the performances of a TEG 27 can be overwhelming because it requires the optimization of many parameters including geometry 28 of heat sinks [2], allocation of heat transfer areas of heat sinks [3-5], dimension of TEG legs [6, 29 7], number of TEG couples [8], and slenderness ratio ((the geometric factor ratio of the n-type to 30 that of the p-type elements)[9]. Nondimensionalization has been performed routinely [10, 11] to 31 reduce the number of design parameters. However, the Thomson effect, which was found to be an 32 essential phenomenon that negatively impacts the maximum power and efficiency [12, 13], was 33 not included in the conventional nondimensionalization. 34 In this work, a new dimensionless number called the Ury number (Ur) is introduced to capture the 35 influence of the Thomson effect. Ur is defined as the ratio between the Thomson coefficient to the 36 Seebeck coefficient. The maximum efficiency and power are redefined with respect to the device 37 figure of merit, ZT, temperature ratio,  $\theta$ , and Ur. It is shown that both the maximum efficiency and 38 power reduce as Ur increases. In the absence of the Thomson effect (Ur=0), the maximum 39 efficiency reverts to the well-known formula for TEG maximum efficiency. Compared with Ur=0, 40 the optimal external load for maximum power stays the same while the optimal external load for 41

the maximum efficiency slightly shifts to a smaller value.

- This article is organized as follows. A mathematical analysis of the governing equations of a TEG is first performed to obtain the equations for the maximum power and maximum efficiency of a TEG. Next, the maximum power and maximum efficiency are optimized through nondimensionalization with various values including the figure of merit of the device, ZT, the temperature ratio between the cold side and hot side temperatures,  $\theta$ , and Ur. Finally, the newly
- derived dimensionless power is validated with experimental data and a detailed discussion on the
- 49 influence of Ur on the maximum power and maximum efficiency for various  $\theta$  and ZT values is
- 50 presented in the results and discussion section.

### 51 Nomenclature

- 52 *A*: Area (m<sup>2</sup>)
- 54 K: Thermal conductance (WK<sup>-1</sup>)
- 55 k: Thermal conductivity (Wm<sup>-1</sup>K<sup>-1</sup>)
- 56 *L*: Length (m)
- 57 N: Number of pairs of p-type and n-type semiconductors
- 58 Q: Heat flow rate (W)
- R: Electrical resistance (Ω), Thermal resistance (KW<sup>-1</sup>)
- 60 S: Seebeck Coefficient (VK<sup>-1</sup>)
- 61 *s*: Entropy (JK<sup>-1</sup>)
- 62 T: Temperature (K)

03	x. Coordinate	
64	Ur: Ury number	
65	W: Power output (W)	
66	ZT: Figure of merit of the TEG	
67	Greek Letters:	
68	$\eta$ : Efficiency	
69	$\mu$ : Thomson coefficient (VK <sup>-1</sup> )	
70	$\theta$ : the ratio between the cold side and hot side temperature	
71	$ ho$ : Electrical resistivity ( $\Omega$ m)	
72	$\dot{\sigma}$ : Rate of entropy generation (WK <sup>-1</sup> )	
73	Subscripts:	
73 74	Subscripts:  c: Cold junction	
74	c: Cold junction	
74 75	c: Cold junction  eff: Effective properties	
74 75 76	c: Cold junction  eff: Effective properties  h: Hot junction	
74 75 76 77	<ul> <li>c: Cold junction</li> <li>eff: Effective properties</li> <li>h: Hot junction</li> <li>in: Input</li> </ul>	
74 75 76 77 78	<ul> <li>c: Cold junction</li> <li>eff: Effective properties</li> <li>h: Hot junction</li> <li>in: Input</li> <li>j: Joule heat</li> </ul>	
74 75 76 77 78 79	c: Cold junction  eff: Effective properties  h: Hot junction  in: Input  j: Joule heat  out: Output	

x: Coordinate

## 82 *th*: thermal

#### 83 Method

# 84 Mathematical Analysis

- 85 Figure 1 shows the schematic of a 1-D TEG along with the thermal resistance network. The
- 86 thermal resistance of the p-type and n-type legs has been considered. Heat loss due to radiation,
- 87 conduction, and convection within the air gap of TEGs was found to have much less impact on
- TEG performance as compared with Thomson effect [14] and is, therefore, neglected in this study.
- 89 The temperature dependent thermoelectric (TE) material properties, including the Seebeck
- 90 coefficient, Thompson coefficient, thermal conductivity, and electrical resistivity, are integrated
- 91 over the temperature gradient and normalized over the temperature gradient to obtain the effective
- 92 TE properties as follow:

$$S_{p,eff} = \frac{\int_{T_c}^{T_h} S_p(T) dT}{T_h - T_c} \tag{1}$$

93

$$S_{n,eff} = \frac{\int_{T_c}^{T_h} S_n(T) \ dT}{T_h - T_c}$$
 (2)

94

$$\mu_{p,eff} = \frac{\int_{T_c}^{T_h} \mu_p(T) \ dT}{T_h - T_c}$$
 (3)

95

$$\mu_{n,eff} = \frac{\int_{T_c}^{T_h} \mu_n(T) \ dT}{T_h - T_c} \tag{4}$$

96

- Where  $\mu$  is the Thomson coefficient obtained through the second Kelvin relationship [15-18] as
- shown in Equation (5). A constant Seebeck coefficient leads to a zero Thomson coefficient.

Commented [ZT1]: I suggest adding a space or , in between consistently to be clearer. As p and eff are two different words

Commented [EK2R1]: Sure

$$\mu = T \frac{dS}{dT} \tag{5}$$

$$k_{p,eff} = \frac{\int_{T_c}^{T_h} k_p(T) \ dT}{T_h - T_c} \tag{6}$$

$$k_{n,eff} = \frac{\int_{T_c}^{T_h} k_n(T) \ dT}{T_h - T_c} \tag{7}$$

$$\rho_{p,eff} = \frac{\int_{T_c}^{T_h} \rho_p(T) \ dT}{T_h - T_c} \tag{8}$$

$$\rho_{n,eff} = \frac{\int_{T_c}^{T_h} \rho_n(T) \ dT}{T_h - T_c} \tag{9}$$

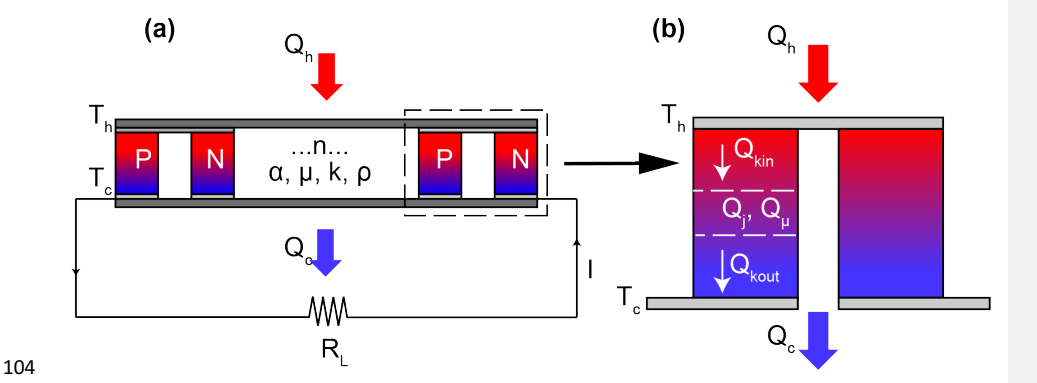


Figure 1: (a) 1-D schematic of a multi-element TEG and (b) heat transfer within a TEG single pair

Figure 1 (a) shows a one-dimensional schematic of a TEG composed of multiple couples of p-type and n-type semiconductors connected electrically in series through strips made of copper and

sandwiched between two plates usually made of Alumina. Figure 1(b) depicts a single TEG couple extracted to show the heat transfer within TEG. When energy balance is performed on the control volume within the single TEG, the heat absorbed at the hot side and heat rejected at the cold side are both found to be as follow:

$$Q_h = SIT_h - 0.5I^2R - 0.5I\mu(T_h - T_c) + K(T_h - T_c)$$
 (10)

$$Q_c = SIT_c + 0.5I^2R + 0.5I\mu(T_h - T_c) + K(T_h - T_c)$$
 (11)

- where the Seebeck coefficient S, Thompson coefficient  $\mu$ , electrical resistance R, and thermal conductance K are respectively defined as:
- $S = S_{p,eff} S_{n,eff} \tag{12}$

$$\mu = \mu_{p,eff} - \mu_{n,eff} \tag{13}$$

$$R = \frac{\rho_{p,eff}L_p}{A_p} + \frac{\rho_{n,eff}L_n}{A_n} \tag{14}$$

$$K = \frac{k_{p,eff}A_p}{L_p} + \frac{k_{n,eff}A_n}{L_n} \tag{15}$$

- 123 TEG produces power through the temperature gradient maintained along the p-type and n-type
- semiconductors which qualify it to be a heat engine. Figure 2 depicts the TEG as a heat engine
- that generates power by acquiring heat from the hot reservoir and dumping the heat that cannot
- be transformed into power to the cold reservoir.

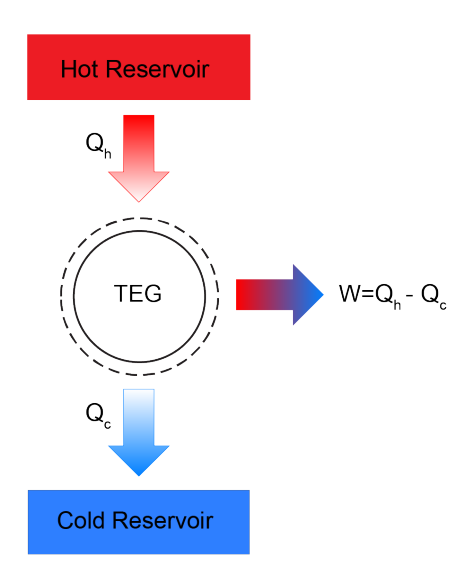


Figure 2: TEG undergoing a power cycle by exchanging heat transfer between two reservoirs

Deleted: 23

128 129

The entropy rate balance of the TEG system represented in figure 4 is:

$$\frac{ds}{dt} = \sum_{j} \frac{Q_j}{T_j} + \dot{\sigma} \tag{16}$$

131

For a steady state, the entropy balance becomes:

$$\dot{\sigma} = -\frac{Q_h}{T_h} + \frac{Q_c}{T_c} \tag{17}$$

133

134 TEG power generation is expressed in terms of entropy as follow:

$$W = Q_h - Q_c = \left(1 - \frac{T_c}{T_h}\right)Q_h - T_c\dot{\sigma} \tag{18}$$

- Also, the power generated by the TEG can be expressed as the difference between the heat
- absorbed and heat rejected as shown in the following expression

$$W = Q_h - Q_c = SI(T_h - T_c) - I^2 R - \mu I(T_h - T_c)$$
 (19)

When the power is divided by the current, the following total voltage expression is obtained

$$V = S(T_h - T_c) - IR - \mu(T_h - T_c)$$
 (20)

- Where the expressions on the right side of Equation (20) are respectively the voltage induced by
- the Seebeck effect, the voltage generated across the p and n-type legs as described by the Ohm's
- Law, and the voltage produced through the Thomson effect.
- Also, the power can be expressed in terms of the external resistance as follow

$$W = Q_h - Q_c = I^2 R_L \tag{21}$$

- where the current I is a function of the Seebeck coefficient S, the Thomson coefficient  $\mu$ , the hot
- and cold side temperatures,  $T_h$  and  $T_c$ , the electrical resistance R, and the external load resistance
- 148  $R_L$ , as shown in Equation (22).

136

139

141

$$I = \frac{(S - \mu)(T_h - T_c)}{R_L + R}$$
 (22)

149 Substituting Equation (22) into Equation (21),

$$W = \frac{(S - \mu)^2 (T_h - T_c)^2}{(R_L + R)^2} R_L$$
 (23)

$$\eta = \frac{W}{Q_h} = \frac{I^2 R_L}{SIT_h - 0.5I^2 R - 0.5I\mu(T_h - T_c) + K(T_h - T_c)}$$
(24)

151 Substituting Equation (22) in Equation (24), the efficiency becomes a

$$\eta = \frac{(S - \mu)(T_h - T_c)R_L}{ST_h(S - \mu)(R_L + R) - 0.5(S - \mu)^2(T_h - T_c)R - 0.5\mu(S - \mu)(T_h - T_c)(R_L + R) + K(R_L + R)^2}$$
(25)

# 153 Power and efficiency optimization

154 Power maximization

152

157

159

- The optimum external load resistance,  $R_L$ , that yields the maximum power of a given TEG at fixed
- 156 hot and cold junction temperatures can be obtained as follow:

$$\frac{\partial W}{\partial R_L} = 0 \tag{26}$$

Determining the optimum value of the external resistance to maximize the power leads to:

$$(R_L)_{opt} = R \tag{27}$$

- 160 The maximum power occurs when the external resistance is equal to the internal resistance of the
- 161 TEG and replacing Equation (27) into Equation (23) yields to the maximum power expressed as:

$$W_{max} = \frac{(S - \mu)^2 (T_h - T_c)^2}{4R}$$
 (28)

$$W_{max}^* = \frac{W_{max}}{KT_c} = \frac{(1-\theta)^2 ZT}{2(1+\theta)\theta} (1-Ur)^2$$
 (29)

where Ur and  $\theta$  are respectively defined as follow:

$$Ur = \frac{\mu}{S} \tag{30}$$

$$\theta = \frac{T_c}{T_h} \tag{31}$$

and ZT is the figure of merit of a TEG device evaluated at the average temperature between the

hot and cold side temperatures

164

166

167

170

172

175

$$ZT = \frac{S^2}{RK} \left( \frac{T_h + T_c}{2} \right) \tag{32}$$

Equation (29) is the dimensionless number that evaluates the effect of Ur,  $\theta$ , and ZT on the

maximum power at optimum  $R_L$ . To evaluate the effect of  $R_L$  on the overall power, a new

173 dimensionless power that contains a dimensionless external resistance would be needed.

174 If  $R^*$  defines the dimensionless external electrical resistance as follow:

$$R^* = \frac{R_L}{R} \tag{33}$$

176 A dimensionless power is obtained as:

$$W^* = \frac{W}{KT_c} = \frac{2ZT(1-\theta)^2(1-Ur)^2}{\theta(1+\theta)(R^*+1)^2}R^*$$
 (34)

- However, the value of the maximum power depends on ZT, Ur, and  $\theta$ .
- 179 Efficiency maximization

182

- The optimum external load resistance,  $R_L$ , that yields to the maximum efficiency of a given TEG
- at fixed hot and cold junction temperatures can be obtained from

$$\frac{\partial \eta}{\partial R_L} = 0 \tag{35}$$

- 183 For maximum efficiency, the obtained result from Equation (35) shows that the external resistance
- 184 needs to be equal to:

$$(R_L)_{opt} = R\sqrt{1 + ZT - ZT \times Ur}$$
(36)

- 186 Note that the optimum external resistance in Equation (36) that maximizes the efficiency is
- different from the one that maximizes the power, Equation (27). Therefore, maximum power and
- 188 efficiency cannot occur at the same optimum external resistance.
- 189 Replacing Equation (36) into Equation (25) and nondimensionalizing the obtained expression
- provides the maximum TEG efficiency as depicted in Equation (38)

$$= \frac{(S-\mu)^2 (T_h - T_c) R_L}{S T_h (S-\mu) (R_L + R) - 0.5 (S-\mu)^2 (T_h - T_c) R - 0.5 \mu (S-\mu) (T_h - T_c) (R_L + R) + K (R_L + R)^2} \Big|_{R_L = R_{L,opt}}$$
(37)

$$\eta_{max}^* = \frac{2ZT(1 - Ur)^2(1 - \theta)\psi}{2ZT(1 - Ur)(1 + \psi) - ZT(1 - Ur)^2(1 - \theta) - ZT * Ur(1 - Ur)(1 - \theta)(1 + \psi) + (1 + \theta)(1 + \psi)^2}$$
(38)

194 where

$$\psi = \sqrt{1 + ZT - ZT \times Ur} \tag{39}$$

To evaluate the effect of the external resistance on the overall efficiency a new dimensionless efficiency is introduced using a dimensionless external resistance  $R^*$ . Incorporating  $R^*$  in the nondimensionalization of the efficiency expression defined in Equation (25), yields to:

$$= \frac{(1 - Ur)(1 - \theta)R^*}{(R^* + 1)\left(1 - \frac{0.5(1 - Ur)(1 - \theta)}{(R^* + 1)} - 0.5Ur(1 - \theta) + \frac{(1 + \theta)(R^* + 1)}{2ZT(1 - Ur)}\right)}$$
(40)

# Results and discussion

The accuracy of the dimensionless expressions introduced in this study is first evaluated by comparing theoretical results with experimental data reported in [19]. In reality, the Ury number varies between 0-1, i.e., 0<Ur<1. For power generation to occur, a positive voltage needs to be inducted, which means that the voltage induced by the Seebeck effect needs to be higher than the sum of the voltage generated by the Thomson effect and Ohm's Law as shown in Equation (20). Therefore, Ur is always smaller than 1. Ur=0 occurs when a constant Seebeck coefficient is assumed in the analysis which leads to a Thomson coefficient equating to zero according to Equation (5). Consequently, TEG power and efficiency are overestimated due to the omission of the Thomson coefficient in TEG power and efficiency expressions, The experimental investigation was performed on TEGs made of bismuth telluride[20]. A TEG made of bismuth telluride typically

operates at a temperature range of 298K-353K. The temperature dependent Seebeck and

Deleted: and has an Ur of 0.42 as detailed below

Deleted:

Thompson coefficients of bismuth telluride are:

$$S_p = (22224 + 930.6T - 0.9905T^2) * 10^{-9}(VK^{-1})$$
(41)

213

$$S_n = -(22224 + 930.6T - 0.9905T^2) * 10^{-9}(VK^{-1})$$
 (42)

214

$$\mu_p = T \frac{dS_p}{dT} (VK^{-1}) \tag{43}$$

215

$$\mu_n = T \frac{dS_n}{dT} \left( V K^{-1} \right) \tag{44}$$

216

- 217 For a better approximation of the Seebeck and Thompson coefficients, they are both integrated
- and normalized over the temperature gradient

$$S_{p,eff} = \frac{\int_{298}^{353} S_p(T) dT}{353 - 298} = 2.2 \times 10^{-4} (VK^{-1})$$
 (45)

219

$$S_{n.eff} = \frac{\int_{298}^{353} S_n(T) dT}{353 - 298} = -2.2 \times 10^{-4} (VK^{-1})$$
(46)

$$\mu_{p,eff} = \frac{\int_{298}^{353} \mu_p(T) dT}{353 - 298} = 9.3 \times 10^{-5} (VK^{-1})$$
(47)

 $\mu_{n,eff} = \frac{\int_{298}^{353} \mu_n(T) dT}{353 - 298} = -9.3 \times 10^{-5} (VK^{-1})$  (48)

 $S = S_{p,eff} - S_{n,eff} = 4.4 \times 10^{-4} \ (VK^{-1})$ (49)

$$\mu = \mu_{p,eff} - \mu_{n,eff} = 18.6 \times 10^{-5} \, (VK^{-1}) \tag{50}$$

 $Ur = \frac{\mu}{S} = 0.42 \tag{51}$ 

Deleted: found

The <u>calculated</u> Ur value <u>of 0.42</u> is far from zero and needs to be included in both maximum and efficiency expressions to accurately represents both TEG power and efficiency. To obtain the dimensionless power data from the experiment, the measured power was divided by the product of the thermal conductance and measured cold side temperature. The theoretical dimensionless power was calculated using Equation (29) where Ur,  $\theta$ , and ZT were calculated from Equation (30), (31), and (32), respectively. Table (1) contains TEG dimensions and operating temperature ranges used in calculating  $\theta$  and ZT.

Table 1: TEG Dimensions and operating temperature ranges

Material	Module Dimensions(mm)	Pellet Dimension (mm)	Couple Number	$T_h$ (°C)	$T_c(^{\circ}C)$
$Bi_2Te_3$	$62 \times 62 \times 5.2$	$4.5 \times 4.5 \times 2.5$	49	100 - 200	37

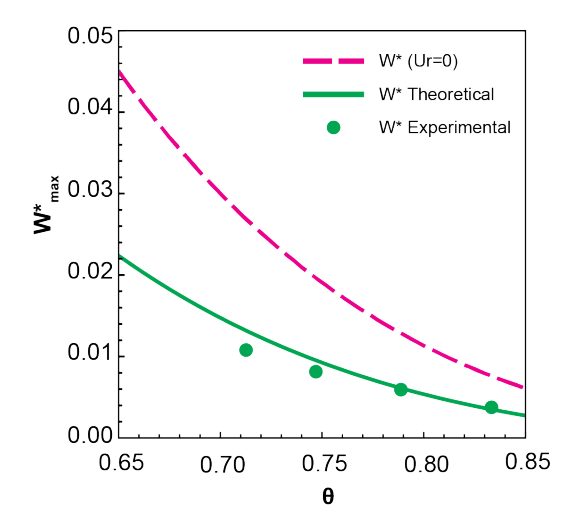


Figure 3: Theoretical and experimental dimensionless power output of bismuth telluride thermoelectric generator device. At θ= {0.698851, 0.73253, 0.773537, 0.817204}, the corresponding Ur= {0.317917, 0.343264, 0.370038, 0.394554}

Both theoretical and experimental dimensionless powers as a function of temperature ratio are plotted in figure 3, and the dimensionless power derived in this study agrees well with the experimental results. As  $\theta$  decreases, which means the temperature gradient increases, the theoretical curve becomes slightly different from the experimental results because the average material properties used in the Ur and ZT calculations deviate more from the actual temperature-dependent material properties at larger temperature gradients. The power production is significantly overestimated at Ur=0 due to the omission of the Thomson effect. Because the Thompson effect induces negative voltage, it reduces the overall TEG voltage across the p-type and n-type semiconductors as shown in Equation (20). As a result, TEG power decreases, Figure

3 shows how the inclusion of Ur into the dimensionless maximum power provides a much better

Deleted:

Deleted: and

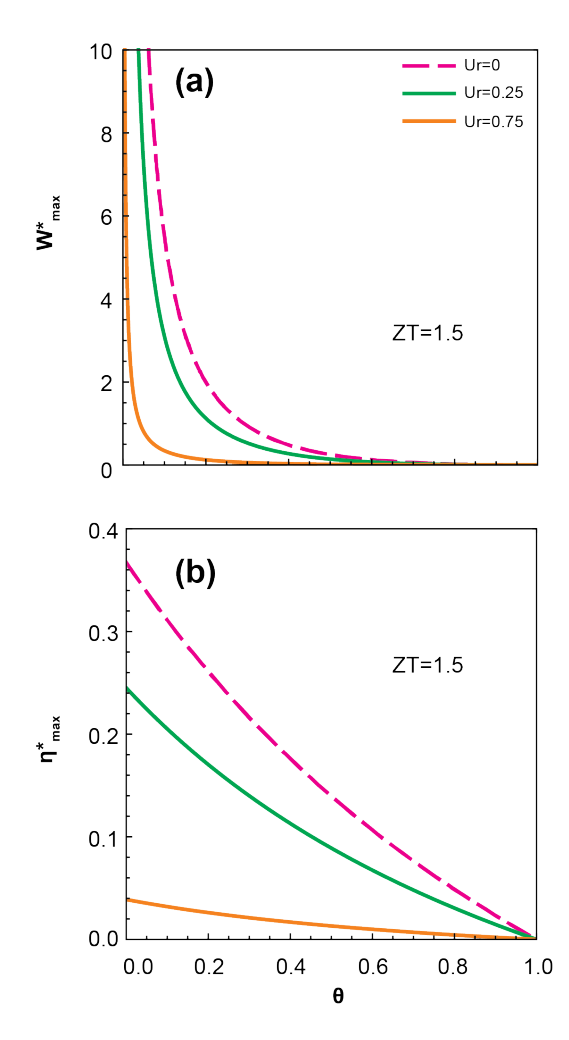


Figure 4: As a function  $\theta$ , for different Ur values and at ZT of 1.5 (a) Variation of the maximum power (b) Variation of the maximum efficiency

262 Ur i 263 to l 264 (2); 265 the 266 sub	gure 4 (a) shows the variation of the dimensionless maximum power with respect to $\theta$ for various numbers at ZT=1.5. All the dimensionless maximum power curves decrease as $\theta$ increases due lower power generation resulting from lower temperature gradients. Referring back to Figure 3; a more significant temperature gradient means that TEG receives more amount of heat from hot reservoir and rejects less amount of heat to the cold reservoir, which generates a more estantial power. Figure 4 (b) shows the maximum dimensionless efficiency with respect to $\theta$ for	Deleted: than received
262 Ur i 263 to l 264 (2); 265 the 266 sub	numbers at ZT=1.5. All the dimensionless maximum power curves decrease as $\theta$ increases due lower power generation resulting from lower temperature gradients. Referring back to Figure ; a more significant temperature gradient means that TEG receives more amount of heat from hot reservoir and rejects less amount of heat to the cold reservoir, which generates a more	Deleted: than received
263 to l 264 (2); 265 the 266 sub	lower power generation resulting from lower temperature gradients. Referring back to Figure ; a more significant temperature gradient means that TEG receives more amount of heat from hot reservoir and rejects less amount of heat to the cold reservoir, which generates a more	Deleted: than received
264 (2); 265 the 266 sub	; a more significant temperature gradient means that TEG receives more amount of heat from hot reservoir and rejects less amount of heat to the cold reservoir, which generates a more	Deleted: than received
265 the 266 sub	hot reservoir and rejects less amount of heat to the cold reservoir, which generates a more	Deleted: than received
266 sub		Deleted: than received
-	stantial power. Figure 4 (b) shows the maximum dimensionless efficiency with respect to $\theta$ for	
267 diff		
	ferent values of Ur. For a given Ur, the maximum efficiency reduces with increasing $\theta$ because	Deleted: each
268 the	maximum power decreases with decreasing temperature gradient. At the same $\theta$ , the maximum	
269 effi	iciency decreases as Ur increases due to the Thomson effect. The negative voltage generated by	
270 the	Thomson effect can be transformed into heat and dissipated out of the p-type and n-type pellets.	Deleted: being
271 Wh	nen part of the heat acquired from the hot reservoir becomes lost to the environment along	
272 <u>pell</u>	lets, it reduces the amount of heat that could have been transformed into useful TEG power and	<b>Deleted:</b> the length of the p-type and n-type semico
273 con	sequently decreases the efficiency. The smaller decay slope of the larger Ur curves indicates	
274 that	t the efficiency becomes less sensitive to operating $\theta$ when the Thomson effect is introduced.	
275 <u>W</u> h	nen Ur=0, both curve falls on top of the calculated curve in Ref. [10], where the Thomson effect	Deleted: ,
276 was	s not taken into account. Because the Thomson effect lowers the power output and efficiency	Deleted: and w
277 for	various $\theta$ , devising ways to reduce the Thomson effect will lead to higher TEG power and	
	iciency.	

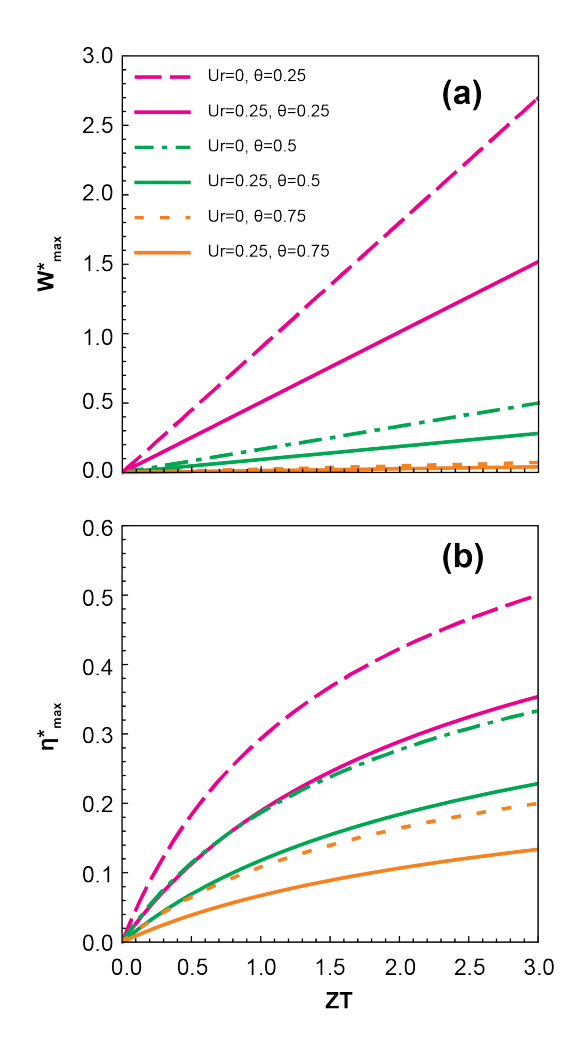


Figure 5: As function of ZT and for different  $\theta$  and Ur values (a) Variation of the maximum power and (b) Variation of the maximum efficiency

Figure 5 (a) shows the variation of the dimensionless maximum power with respect to ZT for different  $\theta$ s and Urs. The dimensionless maximum power increases linearly with increasing ZT for all the cases. This linear behavior is guaranteed by Equation (29). At given  $\theta$  and Ur, the dimensionless maximum power is a linear function of ZT with a constant coefficient of

 $\frac{(1-\theta)^2}{2(1+\theta)\theta}(1-Ur)^2$ . When Ur=0, the curves in Figure 5 (a) become the same as the ones in [10]. 292 The figure of merit, ZT, indicates the ability of a TEG in effectively transforming heat supplied 293 294 form the hot reservoir into power, and a higher ZT lead to higher TEG power and efficiency. A high ZT values requires a large Seebeck coefficient that ties to higher positive voltage which 295 296 contributes to higher TEG power and efficiency, a small thermal conductance to maintain large 297 temperature gradients and reduce heat loss, and a small electric resistance to increase electric 298 current. At a given  $\theta$ , the maximum power output of Ur=0.25 is much lower than that with Ur=0. At lower  $\theta$ , the difference between Ur=0.25 and Ur=0 is more significant. In other words, power 299 reduction by Thomson effect is more significant at larger temperature gradients because of larger 300 301 Thomson coefficient. Figure 5 (b) shows the maximum dimensionless efficiency as a function of ZT for different θs and Ur numbers. The maximum efficiency increases with increasing ZT at 302 303 given Ur and  $\theta$ , and it will approach a plateau. At a given  $\theta$ , the maximum efficiency is reduced as Ur increases. This reiterates how the Thomson effect significantly reduces the efficiency of a TEG. 304

Deleted: The physical explanation of higher ZT leading to higher power and efficiency production corresponds to higher Seebeck coefficient that ties to higher positive voltage which contributes to higher TEG power and efficiency. Nevertheless, increasing ZT implies reducing the electrical resistance and thermal conductance across the ZT as shown in Equation (32). As explained earlier, a higher temperature across TEG generates more power and in order for this to occur the thermal conductance needs to be reduced to prevent heat being transferred along the p-type and n-type, and the electric resistances of the p-type and n-type pellets need to be minimum to increase electric current flow.

Commented [ZT3]: Isn't this because of the definition of Thomson coefficient? Small temperature gradient, not much change in S, small Thomson coefficient

Commented [EK4R3]: yes

Deleted: shows

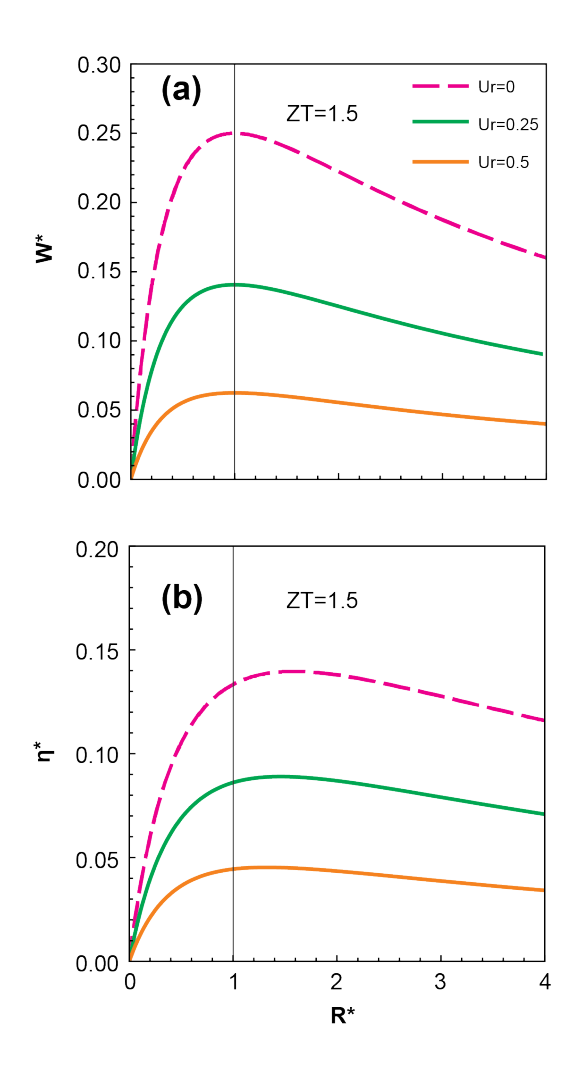


Figure 6: As a function of  $R^*$ , at a  $\vartheta$  of 0.5, and for various Ur values (a) Dimensionless power and (b) Dimensionless efficiency

Figure 6 (a) and (b) shows the variation of the dimensionless power  $W^*$  and efficiency  $\eta^*$  as a

function of the dimensionless external resistance  $R^*$ . As Ur increases, both power and efficiency are reduced due to the Thomson physical phenomenon.

The optimum  $R^*$  for maximum power is always 1 as opposed to the optimum  $R^*$  for maximum 323 efficiency that occurs at a value of  $R^*\sqrt{1+ZT-Ur\times ZT}$ . Taking the case when Ur=0.25, the 324 optimum  $R^*$  for maximum efficiency is 1.32, Note that when dealing with a TEG composed of 325 multiple pellets, the electrical resistance adds up leading to a significant difference between the 326 external resistance that will maximizes the power and efficiency. For example, if TEG internal 327 328 electric resistance of multiple pellets is  $20\Omega$ , the optimum external resistance for power will remain 329  $20\Omega$  while  $26.4\Omega$  is required for maximum efficiency. The dimensional electrical resistance is an excellent parameter to guide TEG design towards maximization of power or efficiency. 330 Conclusion 331

Nondimensionalization of the output power and the efficiency of a TEG is revisited with the inclusion of the Thomson effect. The Ury number (Ur) that describes the ratio between Thomson and Seebeck coefficients is introduced. Ur is the first dimensionless number reported in the literature that quantifies the relative importance of the Thomson effect. When Ur is nonzero, the maximum power output and efficiency are reduced from those with Ur=0. The findings obtained from this study can be summarized as follow:

332

333

334

335

336

337

338

339

340

341

342

343

344

- The negative impact of the Thomson effect on TEG power and efficiency is captured by reformulating the maximum power and thermoelectric efficiency formula via the introduction of a new dimensionless number called the Ury number (Ur).
- The theoretical results are validated with experimental data, and it is found that without
  the inclusion of Thomson coefficient through the Ury number, TEG power can be
  significantly overestimated, which suggests that Ury is a crucial number in predicting
  accurate TEG experimental data.

Deleted: , which is close to 1

Deleted: However

Deleted:

- The maximum power occurs when the external resistance is equal to the internal resistance of the TEG while the maximum efficiency happens when the external resistance is equivalent to  $(R_L)_{opt} = R\sqrt{1 + ZT Ur \times ZT}$ .
- The revised dimensionless maximum power and efficiency are now functions of both ZT
  and Ur, which better agreement with the experimental data and developing strategies to
  reduce the Thomson effect will lead to TEG better performances.

## 354 Acknowledgments

- 355 This work was funded by Z.T.'s startup fund from Virginia Polytechnic Institute and State
- 356 University and Z.T.'s NSF CAREER award NSF CAREER Award (CBET-1839384).

#### 357 References

- 1. Nolas, G.S., J. Sharp, and J. Goldsmid, *Thermoelectrics: basic principles and new materials developments.* Vol. 45. 2013: Springer Science & Business Media.
- Wang, C.-C., C.-I. Hung, and W.-H. Chen, Design of heat sink for improving the
   performance of thermoelectric generator using two-stage optimization. Energy, 2012.
   39(1): p. 236-245.
- 36. Luo, J., et al., Optimum allocation of heat transfer surface area for cooling load and
  364 COP optimization of a thermoelectric refrigerator. Energy conversion and management,
  365 2003. 44(20): p. 3197-3206.
- Chen, L., et al., Performance optimization of a two-stage semiconductor thermoelectricgenerator. Applied Energy, 2005. 82(4): p. 300-312.
- Chen, L., F. Meng, and F. Sun, Effect of heat transfer on the performance of
   thermoelectric generator-driven thermoelectric refrigerator system. Cryogenics, 2012.
   52(1): p. 58-65.
- Yazawa, K. and A. Shakouri, Optimization of power and efficiency of thermoelectric
   devices with asymmetric thermal contacts. Journal of Applied Physics, 2012. 111(2): p.
   024509.
- Mayer, P. and R. Ram, Optimization of heat sink-limited thermoelectric generators.
   Nanoscale and Microscale Thermophysical Engineering, 2006. 10(2): p. 143-155.
- 376 8. Chen, L., et al., Effect of heat transfer on the performance of thermoelectric generators.
  377 International journal of thermal sciences, 2002. 41(1): p. 95-99.
- Yilbas, B. and A. Sahin, Thermoelectric device and optimum external load parameter
   and slenderness ratio. Energy, 2010. 35(12): p. 5380-5384.
- Sahin, A.Z. and B.S. Yilbas, The influence of operating and device parameters on the maximum efficiency and the maximum output power of thermoelectric generator.
   International Journal of Energy Research, 2012. 36(1): p. 111-119.

- Lee, H., Optimal design of thermoelectric devices with dimensional analysis. Applied
   energy, 2013. 106: p. 79-88.
- Chen, J., Z. Yan, and L. Wu, The influence of Thomson effect on the maximum power
   output and maximum efficiency of a thermoelectric generator. Journal of applied physics,
   1996. 79(11): p. 8823-8828.
- 388 13. Kanimba, E., et al., *A modeling comparison between a two-stage and three-stage cascaded thermoelectric generator.* Journal of Power Sources, 2017. **365**: p. 266-272.
- Kanimba, E., et al., A comprehensive model of a lead telluride thermoelectric generator.
   Energy, 2018. 142: p. 813-821.
- Ioffe, A., Kaye, J. and Welsh, JA Direct Conversion of Heat to Electricity. John Wiley
   and Sons, Inc., 1960.
- 394 16. Sutton, G.W., Direct energy conversion. 1966.
- 17. Decher, R., Direct Energy Conversion: fundamentals of electric power production. 1997:
   Oxford University Press on Demand.
- 397 18. Riffat, S.B. and X.L. Ma, *Thermoelectrics: a review of present and potential applications*. Applied Thermal Engineering, 2003. **23**(8): p. 913-935.
- 399 19. Zhu, J., et al., *Experimental study of a thermoelectric generation system.* Journal of electronic materials, 2011. **40**(5): p. 744-752.
- 401 20. Saleemi, M., et al., Synthesis, processing, and thermoelectric properties of bulk
   402 nanostructured bismuth telluride (Bi 2 Te 3). Journal of Materials Chemistry, 2012.
   403 22(2): p. 725-730.